Imaging Volcanic Eruption Dynamics with WAMS, a Millimeter-wave Radar and Radiometer

Sean Bryan, James Aberle
Senior Member, IEEE,
and Daniel Bliss *Fellow, IEEE*
School of Electrical, Computer
and Energy Engineering
Arizona State University
Tempe, AZ 85283
Email: sean.a.bryan@asu.edu

Amanda Clarke, Christopher Groppi,
and Philip Mauskopf
School of Earth and Space Exploration
Arizona State University
Tempe, AZ 85283

Loÿc Vanderkluysen
Biodiversity, Earth and
Environmental Science Department
Drexel University
Philadelphia, PA 19104

Scott Paine
Center for Astrophysics | Harvard & Smithsonian
Cambridge, MA 02138

***Abstract*—Millimeter-wave radar has the potential to transform measurements of volcanic eruptions by imaging the interior of eruption plumes for the first time. This new kind of data would answer a wide range of fundamental questions about volcanology and multiphase fluid dynamics. Crucially, it also would significantly improve the ability to forecast and mitigate the hazard to aviation caused by volcanic ash clouds. To accomplish this, we are developing the Water and Ash Millimeter-wave Spectrometer (WAMS) instrument. Its 220 GHz FMCW radar system has an operating frequency chosen to maximize the system sensitivity to volcanic ash, and is built entirely from commercial off-the-shelf components.**

I. Introduction

Volcanic eruption plumes are complex multiphase fluid-dynamical systems with a wide range of internal processes such as ash particle production and transport, internal chemical reactions, and shock waves. The large number of processes, and their interactions, make eruptions too complex to fully model in computer simulations or laboratory analogs. Current infrared [1] and optical [2] measurement systems are limited to the outer surface and cannot image the interior of plumes. Open path FTIR [3] can measure internal water vapor and other gases to some degree, but its performance is limited due to saturation at moderate/high concentrations. Centimeter-wave weather radar [4], [5], [6], [7], [8], [9] offers a limited view of ash inside eruptions at low spatial resolution and sensitivity, but like the other existing techniques it utility is limited.

Because of the limitations of simulations, laboratory analogs, and current measurement techniques, the interiors of volcanic eruption plumes remain largely unexplored. This leaves a range of important fundamental questions unanswered, such as: What basic processes control the interior dynamics of eruption plumes? What is the role of turbulence in eruptions, and what turbulent length scales dominate? How do particles move, aggregate, and interact with the rest of the flow? What chemical reactions occur? How do hail, ice, and sulfates form inside eruptions?

In addition to the scientific impact, one practical consquence of resolving these fundamental questions is an improved ability to forecast and mitigate the hazard that volcanic ash clouds cause to global aviation. The 2010 Eyjafjallajökull eruption in Iceland produced volcanic ash that spread through global wind patterns and caused major disruption and hazards to aviation. The event caused the largest disruption to European airspace since WWII. Improved understanding of basic eruption processes, as well as the ability to make realtime measurements of the volume and properties of ash production as input to global ash distribution forecasts, are needed to mitigate future similar eruption events [10], [11].

A millimeter-wave radar system would be uniquely capable of making realtime ash measurements for input to realtime ash hazard forecasts, and resolving the basic volcanology and fluid dynamics science questions. We are therefore developing the Water and Ash Millimeter-Wave Spectrometer (WAMS) instrument [12] with a 220 GHz radar system. Here we present an update on the development status of the project. We verified that our the operating frequency is optimal to image the science target. We also made progress designing the radar chirp parameters, and designing the initial approach for T/R isolation.

II. Radar Signal from Volcanic Ash

A. Why 220 GHz?

Several competing factors determined our selection of 220 GHz as the operating frequency. The radar return, atmospheric attenuation, transmit power of commercially-available power amplifiers, and the system noise temperature of commercially-available mixer receivers, all vary with frequency. This means that achieving the highest system sensitivity will not necessarily mean maximizing any single parameter, but rather will

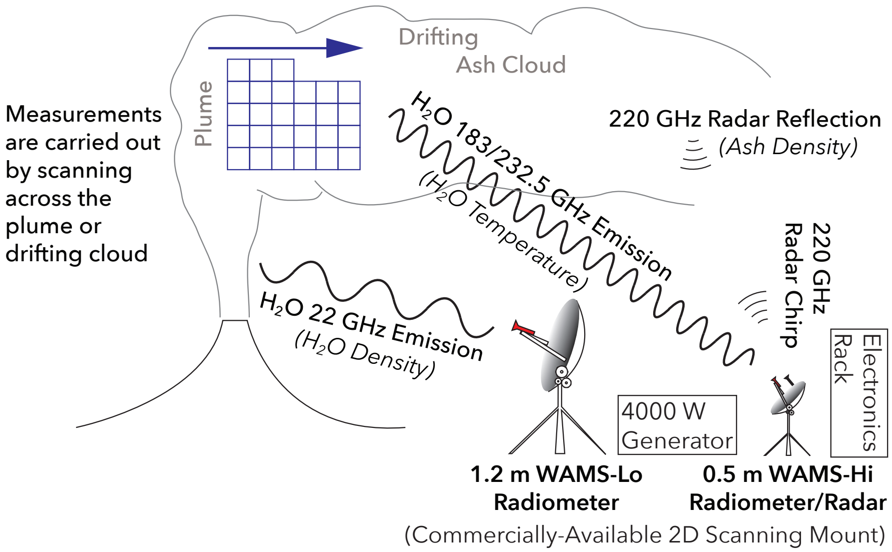

Fig. 1. Illustration of the WAMS instrument concept. Millimeter-wave radar will enable 3D imaging of the fine ash of high-altitude volcanic eruption clouds for the first time. Microwave radiometers at several frequencies will measure the density and temperature distribution of water vapor throughout the eruption. The instrument would be compact enough to be rapidly transported and deployed near an eruption as it happens.

require optimizing the total combination. As an example of how changing the operating frequency changes the overall sensitivity to volcanic ash, consider operating in the 90 GHz atmospheric window instead. VDI makes a 90 GHz transmitter with 800 mW of transmit power, ten times more than our 80 mW 220 GHz transmitter from the same company. At 90 GHz, atmospheric attenuation is slightly better, and receivers with slightly better system noise may also be available. However, for the fine particles in the high altitude volcanic dust cloud, the radar return is significantly smaller at 90 GHz. We discuss the exact radar cross section calculation in the next subsection, but for the moment we assume the scattering is in the Rayleigh limit and scales as λ^{-4}. This means that at 90 GHz the radar return will be dimmer by a factor of $((220\ \text{GHz})/(90\ \text{GHz}))^4 \approx 36$. This is not compensated by the tenfold increase in transmitter power, showing that increasing the operating frequency to 220 GHz significantly improves the system performance.

Increasing the operating frequency above 220 GHz has diminishing returns. At 280 GHz, the atmospheric attenuation is worse than at 220 GHz, catastrophically worse at high humidity. VDI makes a transmitter at 280 GHz with 30 mW of output power, lower by a factor of $(80\ \text{mW})/(30\ \text{mW}) \approx 2.7$. The radar return is larger by almost exactly the same factor, $((280\ \text{GHz})/(220\ \text{GHz}))^4 \approx 2.7$, but increased atmospheric attenuation would make the final system performance somewhat worse. There is not another significant millimeter-wave atmospheric window above 305 GHz to consider. Increasing to the IR/optical window would mean the operating wavelength would no longer be in the Mie resonance region of the larger ash particles, taking away the key ability to measure volcanic ash particle size discussed in the next subsection.

B. Radar Cross Section

As we discussed in an earlier paper [12], ash particles in volcanic eruptions vary by eruption but are often basaltic with a density of 2.3-2.8 g/cm^3, 0.1-2 mm in size, and a measured millimeter-wave dielectric constant of $\epsilon_r = 5.4 - 0.16j$. We used these parameters to calculate the radar cross section, per gram of material, to be 400-1600 mm^2/g at 220 GHz. These particles sizes are in the Mie resonance region for our operating frequency, so we used a full Mie theory numerical code to calculate the cross section without making the optical or Rayleigh approximation. Note also that the large uncertainty in particle size (factor of 20) fortunately does not translate into nearly as large of an uncertainty in radar cross section (only a factor of 4), since we are in the Mie resonance region. This will let us interpret the measured radar signals as a measurement of volcanic ash mass flux, something no other measurement technique can do. Based on typical ash concentrations in eruptions ranging over 1-1000 g/m^3, and the properties of the WAMS radar system observing at 10 km standoff distance, the final calculated [12] radar SNR per volume element is 30-44 dB when integrating for a second. We also have calculated Cramér-Rao bounds on the ultimate performance limit of the system.

Currently it is common to estimate the sizes of volcanic ash particles based on collecting ash samples on the ground after eruptions. This approach is limited because transport through the atmosphere affects different sizes differently. Also, it is believed that finer ash particles are carried into the upper atmosphere and that larger particles settle out, but this effect has not been observed directly in an eruption because it is not possible to measure the ash particle size in situ. A key result of our study [12] of the millimeter wave radar signal from ash is that retuning the radar in realtime will let us measure

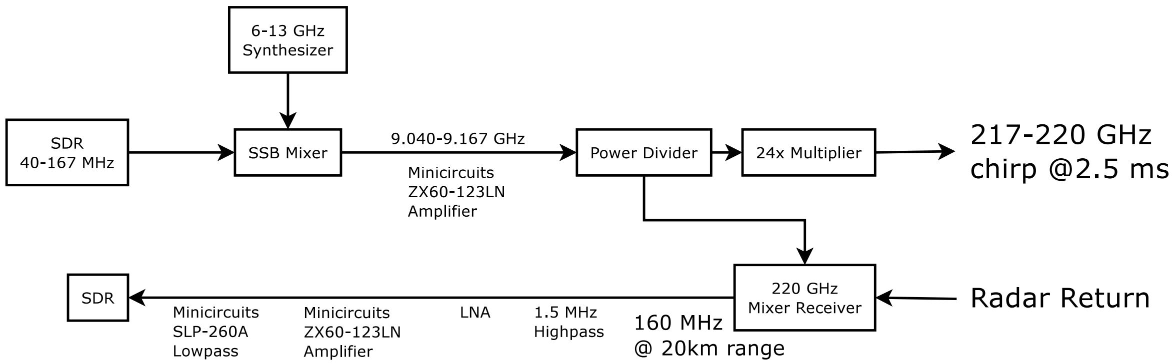

Fig. 2. Flowchart illustrating the signal flow in the WAMS radar system along with selected parts.

the particle size directly, and in different parts of the eruption. Directly measuring the size of the particles in the drifting ash cloud will be key for validating ash transport models used in aviation safety.

III. Instrument Hardware and Operations

When an eruption event occurs, the WAMS system will be shipped to the site. The instrument is small enough to fit in a standard pickup truck, including the standard gas generator used to provide electrical power. The instrument will then be unpacked at a site a safe distance away near the eruption. The single radar beam will repeatedly scan over the eruption creating 3D time-resolved images of the eruption. In a previous paper [12], we showed that the signal will still be observable at at 10-20 km standoff distance, similar to other geology observing practices.

WAMS uses only commercially-available components, integrated with standard WR5 and SMA connectors, to reduce implementation risk and control cost. The 220 GHz radar system is a single-polarization FMCW radar. The chirp signal is synthesized at baseband with a software-defined radio, SSB mixed up to 9 GHz, then multiplied in frequency by 24 and amplified to an output power of 80 mW at 220 GHz with VDI AMC-583 220 GHz transmitter. The signal is then send to one of the linear-polarization inputs of an ASU-fabricated orthomode transducer [13], [14], then coupled to free space through a dual-polarization feed horn [15], [16]. A QMC free-space Faraday rotator will convert this signal to right-circular polarization. The beam will be formed with a 50 cm parabolic reflector and the entire system will scan on a gimbal from RIE Technologies. The reflection from the dielectric target will appear mostly as left-circular polarization traveling back to the radar receiver as the return. The received signal will pass the free space Faraday rotator, converting from left-circular to the other linear polarization. It will enter the feed horn and come out the other port of the orthomode transducer to a VDI MixAMC-293 220 GHz receiver. The FMCW signal will appear at baseband at the output of the receiver, as the result of using the chirp signal as the mixing reference.

The IF ports of the millimeter-wave transmitter and receiver need to be driven by 200 MHz electronics. We plan to use a software-defined radio system such as the academic-developed CASPER-ROACH [17] or the commercial Xilinx RFSoC Evaluation board. The RF ADC will make a FMCW chirp signal from 40 MHz to 167 MHz in 2.5 ms. After multiplication by the VDI transmitter this will be a 3 GHz bandwidth chirp at 220 GHz, yielding a fundamental range resolution of c / (2 $\times$ (3 GHz)) = 5 cm. This will be heavily averaged in realtime FPGA/CPU processing into 60 m range bins to match the cross-range resolution of the beam at 10 km. With this 2.5 ms sweep rage, the 200 m range bin will appear at an IF of 1.6 MHz, just above the IF highpass filter. The 20 km range bin will appear at 160 MHz, the upper end of the RF DAC bandwidth. The radar signal will be further averaged in time. Assuming 1 second interactions, the final data rate of the system will be fairly modest with only 330 60-m range bins from 0.2-20 km recorded to disk every second.

A key consideration in any radar system is the transmitter/receiver isolation. An FMCW system cannot use a T/R switch so here we review the isolation provided by the relevant RF/millimeter-wave components. The OMT has leakage from one input port onto the other. For this specific design, poor isolation arises from slight misalignment between the two mechanical components in the spilt block construction. We simulated both the ideal and misaligned cases in CST for the exact design we plan to use. We found that the worst-case isolation in the misaligned case is 50 dB. Thus, we expect (20 dBm transmit power) - (50 dB OMT isolation) = -30 dBm of power to appear at the receiver input, and the equivalent near DC at the IF output. This will not drive the receiver non-linear because its saturation power is -10 dBm. In out relevant range bins of 0.2-20 km, further isolation will be accomplished by filtering the IF signal with a commercial 1.5 MHz Minicircuits SXHP-2+ highpass filter. This provides -50 dB further isolation, meaning that in the 0.2 km range bin we expect -80 dBm of leakage of transmit power. Across the entire millimeter wave bandwidth, the 2500 K lab-measured system temperature of the receiver translates into $k\times$(3 GHz)$\times$(2500 K) = -70 dBm, meaning that the transmit leakage is expected to be 10 dB below the receiver noise. Verifying that this T/R isolation plan yields good system performance, or modifying the system if it does not, will be a key part of the WAMS development program. Still, this promising initial estimate motivates our selection of this system design and components.

IV. Conclusion

The WAMS instrument will let us take advantage of the unique ability of millimeter-wave radar to measure the interior of eruption plumes. Our 220 GHz operating frequency strikes the optimal balance between available transmitter power, radar return, and atmospheric attenuation, leading us to believe it will yield the best system performance. We calculated that commercially-available components should enable us to achieve the required T/R isolation, with the possibility to modify or replace individual connectorized modules in our system in the future to make further improvements. The data from WAMS will be key in resolving basic science questions in volcanology, and the system also represents an important capability for making realtime measurements as inputs to forecasting volcanic ash hazards to aviation.

References

[1] A. J. L. Harris, S. Valade, G. M. Sawyer, F. Donnadieu, J. Battaglia, L. Gurioli, K. Kelfoun, P. Labazuy, T. Stachowicz, M. Bombrun, V. Barra, D. Delle Donne, and G. Lacanna. Modern multispectral sensors help track explosive eruptions. *Eos, Transactions American Geophysical Union*, 94(37):321–322, 2013.

[2] R. S. J. Sparks and L. Wilson. Explosive volcanic eruptions v. observations of plume dynamics during the 1979 soufrire eruption, st vincent. *Geophysical Journal of the Royal Astronomical Society*, 69(2):551–570, 1982.

[3] Lisa A. Horrocks, Clive Oppenheimer, Michael R. Burton, Hayley J. Duffell, Nicholas M. Davies, Nicholas A. Martin, and William Bell. Open-path fourier transform infrared spectroscopy of so2: An empirical error budget analysis, with implications for volcano monitoring. *Journal of Geophysical Research: Atmospheres*, 106(D21):27647–27659.

[4] D. J. Schneider and R. P. Hoblitt. Doppler weather radar observations of the 2009 eruption of redoubt volcano, alaska. *Journal of Volcanology and Geothermal Research*, 259:133 – 144, 2013.

[5] Stefano Corradini, Mario Montopoli, Lorenzo Guerrieri, Matteo Ricci, Simona Scollo, Luca Merucci, Frank S. Marzano, Sergio Pugnaghi, Michele Prestifilippo, Lucy J. Ventress, Roy G. Grainger, Elisa Carboni, Gianfranco Vulpiani, and Mauro Coltelli. A multi-sensor approach for volcanic ash cloud retrieval and eruption characterization: The 23 november 2013 etna lava fountain. *Remote Sensing*, 8(1):58, 2016.

[6] Masayuki Maki, Masato Iguchi, Takeshi Maesaka, Takahiro Miwa, Toshikazu Tanada, Tomofumi Kozono, Tatsuya Momotani, Akihiko Yamaji, and Ikuya Kakimoto. Preliminary results of weather radar observations of sakurajima volcanic smoke. *Journal of Disaster Research*, 11(1):15–30, 2016.

[7] F. S. Marzano, E. Picciotti, E. Montopoli, and G. Vulpiani. Inside volcanic clouds: Remote sensing of ash plumes using microwave weather radars. *Bulletin of the American Meteorological Society*, 94(10):1567–1586, 2013.

[8] P. Arason, G. N. Petersen, and H. Bjornsson. Observations of the altitude of the volcanic plume during the eruption of eyjafjallajkull, aprilmay 2010. *Earth System Science Data*, 3(1):9–17, 2011.

[9] F. Donnadieu, G. Dubosclard, R. Cordesses, T. Druitt, C. Hervier, J. Kornprobst, J.-F. Lnat, P. Allard, and Mauro Coltelli. Remotely monitoring volcanic activity with ground-based doppler radar. *Eos, Transactions American Geophysical Union*, 86(21):201–204, 2005.

[10] A. R. Van Eaton, L. G. Mastin, M. Herzog, H. F. Schwaiger, D. J. Schneider, K. L. Wallace, and A. B. Clarke. Hail formation triggers rapid ash aggregation in volcanic plumes. *Nature Communications*, 6, Aug 2015.

[11] C. Bonadonna, A. Folch, S. Loughlin, and H. Puempel. Future developments in modelling and monitoring of volcanic ash clouds: outcomes from the first iavcei-wmo workshop on ash dispersal forecast and civil aviation. *Bulletin of Volcanology*, 74(1):1–10, 2012.

[12] S. Bryan, A. Clarke, L. Vanderkluysen, C. Groppi, S. Paine, D. W. Bliss, J. Aberle, and P. Mauskopf. Measuring water vapor and ash in volcanic eruptions with a millimeter-wave radar/imager. *IEEE Transactions on Geoscience and Remote Sensing*, 55(6):3177–3185, June 2017.

[13] T.J. Reck and G. Chattopadhyay. A 600 ghz asymmetrical orthogonal mode transducer. *Microwave and Wireless Components Letters, IEEE*, 23(11):569–571, Nov 2013.

[14] A Navarrini, C. Groppi, and G. Chattopadhyay. A waveguide orthomode transducer for 385-500 ghz. *International Symposium on Spate Terahertz Technology*, 2010.

[15] Boon-Kok Tan, Jamie Leech, Ghassan Yassin, Phichet Kittara, Mike Tacon, Sujint Wangsuya, and Christopher Groppi. A high performance 700ghz feed horn. *Journal of Infrared, Millimeter, and Terahertz Waves*, 33(1):1–5, 2012.

[16] Boon-Kok Tan, G. Yassin, P. Grimes, J. Leech, K. Jacobs, and C. Groppi. A 650 ghz unilateral finline sis mixer fed by a multiple flare-angle smooth-walled horn. *Terahertz Science and Technology, IEEE Transactions on*, 2(1):40–49, Jan 2012.

[17] J. Hickish, Z. Abdurashidova, Z. Ali, K. D. Buch, S. C. Chaudhari, H. Chen, M. Dexter, R. S. Domagalski, J. Ford, G. Foster, D. George, J. Greenberg, L. Greenhill, A. Isaacson, H. Jiang, G. Jones, F. Kapp, H. Kriel, R. Lacasse, A. Lutomirski, D. MacMahon, J. Manley, A. Martens, R. McCullough, M. V. Muley, W. New, A. Parsons, D. C. Price, R. A. Primiani, J. Ray, A. Siemion, V. van Tonder, L. Vertatschitsch, M. Wagner, J. Weintroub, and D. Werthimer. A Decade of Developing Radio-Astronomy Instrumentation using CASPER Open-Source Technology. *Journal of Astronomical Instrumentation*.